

Modeling and Simulation of Offshore Wind Farms for Farm Level Control

Mohsen Soltani, Torben Knudsen, Thomas Bak

September 15, 2009

1 Summary

This paper presents a procedure for wind farm model simulation. The simulation model serves as a benchmark for controller development and verification in the EU-FP7 project Aeolus. A generic dynamic flow modeling relates single turbine production and fatigue load to the map of wind speeds. The model integrates the wind farm aerodynamics to the dynamics of individual turbines by means of wake meandering. The model gives engineers the possibility to model different farm size and arrangements. Eventually, the OWEZ offshore wind farm is simulated by this model.

2 Introduction

Wind farm modeling has previously been studied in two aspects; aerodynamic effects and power production and grid integration. The aerodynamic modeling part of the wind farm has been described by wind turbine wakes. There are generally two ways of wake modeling: either using full equation models or using simplified methods (static/quasi-static/dynamic engineering approaches). The power production modeling part was studied to improve the grid integration issue of the wind farm. The purpose of the presented simulation model is to serve as a benchmark for farm controllers controlling the individual turbines in a farm to achieve the farm power set point with smallest possible mechanical loads.

This paper presents the procedure for wind farm modeling. Wind farm modeling is part of the European EU-FP7 project Aeolus [13] with the title "Distributed Control of Large-Scale Offshore Wind Farms". The presented modeling approach maps the aerodynamic specifications of the wind field to the dynamics of wind turbines and the power production at the farm level. In addition, the mapping makes it possible to provide a model for the fatigue loads on individual wind turbines regarding the wake effect in the farm.

In this model the wind field information flows to all wind turbines. This gives us two capabilities. When wind turbines in the upwind row are hit by a large or extreme gust, the traveling of this gust will be modeled and the downwind turbines will be affected. By combining the individual wind turbine information, the model relates power set point changes to wind field changes in the farm. This is of importance when knowing the wind field changes affects the fatigue loads on downstream wind turbines and that in the later stages the total farm power set point has to be met with the smallest possible farm fatigue load.

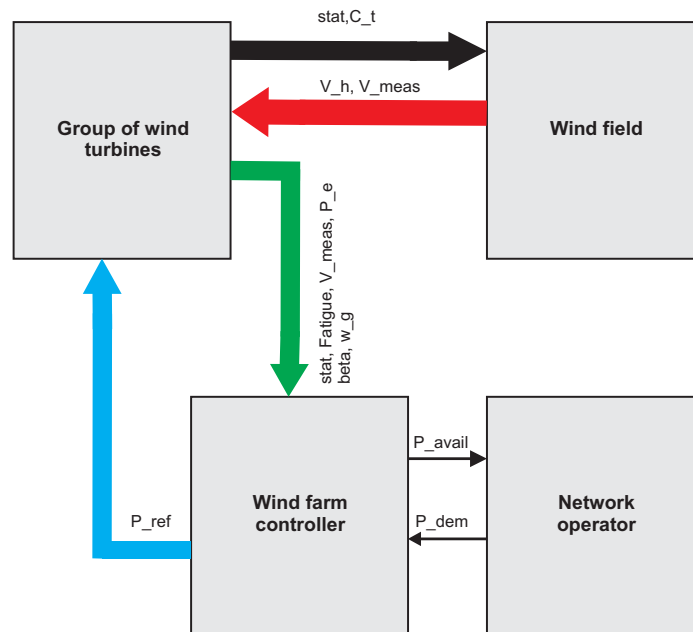


Figure 1: The first level of the wind farm model.

3 Wind Farm Model Structure

The wind farm model includes four major elements: wind turbines, wind field, wind farm controller, and network operator. Figure 1 represents the connections of those components. In this figure, $stat$ is the status of the wind turbine (simply 0/1 when the wind turbine is on/off), C_t is the thrust coefficient, P_e is the produced power, $Fatigue$ is an estimate for the fatigue load, V_{meas} is the measured wind speed on the wind turbine, V_h is the wind speed in the wind field at hub-high, P_{avail} is the available power, P_{dem} is the farm power demand, and P_{ref} is the group of all power references for the wind turbines. Note that in this text, P_{ref} is substituted instead of a variable which is known as the rated power in the single turbine controller.

The electro-mechanical model of the wind turbine together with the individual wind turbine controller is used. The wind turbine itself is an energy transformer with wind energy as input and the produced power as output. The wind turbine also affects the downstream wind which is experienced by other wind turbines in the wind farm (depending on how much energy is absorbed by the wind turbine).

Moreover, one of the objectives of Aeolus [1] is to reduce fatigue loads experienced by wind turbines. The fatigue load is estimated from turbine sensor signals e.g. tower accelerometers [3]. This estimation data has to be used in the wind farm controller and will effect the distribution of the power references on the wind turbines.

The working wind turbines in a wind farm influence each other through the wind field. These effects are mainly due to the wakes behind every wind turbine. The wake model is then used to explain the wind field in a large grid of wind turbines. A simplified analytical methodology is used as an initial point for wind field model in Aeolus. The related works on analysis of the wake deficit [5] is used together with a wake meandering model [14] to achieve the position and deficit of the wakes on all wind turbines. An algorithm regarding the calculations for a computer-based model is given. Then, the wind speed at each wind turbine (hub-high wind speed) is achieved.

The wind farm controller is the interface between the network operator and individual wind turbine

controllers. Its main objective is to provide outputs in two directions; toward the operator and toward the wind farm. The first output is a prediction of the available power at the wind farm. This means that by analyzing the inputs from the wind farm the controller must provide an estimate of the available power in the wind farm to the operator. This is done by simply summing up the available electrical power at each wind turbine which is predicted from the hub-high wind speed or a wind speed estimated based on using the turbine as a measurement device. The second output is the group of power references for individual wind turbine controllers. This power reference will be produced for each wind turbine by analysing the fatigue load and produced power compared to the total farm power demand from the network operator.

The network operator provides the power demand for the wind farm controller. This demand could be categorized in different modes [2, 8]. The detail description of the wind farm components are given in the following sections.

3.1 Wind Turbine

The main components of the wind turbine model are aerodynamics, drive train, tower, generator, pitch actuator, and the wind turbine controller (see figure 2). When wind passes the wind turbine rotor plane, part of the kinetic energy in the wind is transferred to the rotor. The power P_a obtained by the rotor is given by [9]

$$P_a = \frac{\pi}{2} \rho R^2 v_r^3 C_P(\lambda, \beta), \quad (1)$$

where ρ is the air density, R is the rotor radius, v_r is the effective wind speed on the rotor, and C_P is the power efficiency coefficient (For more details see [3]). In addition to delivering power to the wind turbine, the wind will exert a thrust on the rotor plane which is a force on the rotor in the fore-aft direction. The thrust force F_t is given by

$$F_t = \frac{\pi}{2} \rho R^2 v_r^2 C_T(\lambda, \beta). \quad (2)$$

As indicated, the coefficients C_P and C_T are both functions of the tip speed-ratio λ and the blade pitch angle β with tip speed-ratio defined as

$$\lambda = \frac{\omega_r R}{v_r}. \quad (3)$$

Finally, as the rotor power P_a and rotor torque T_a are related to rotor angular rotational speed ω_r as $P_a = T_a \omega_r$, we have for the aerodynamic torque:

$$T_a = \frac{\pi}{2 \omega_r} \rho R^2 v_r^3 C_P(\lambda, \beta). \quad (4)$$

In the simulation model, the aerodynamics block complies with the above description. The C_P and C_T are found from the lookup tables for the given β and λ and finally the thrust force and the aerodynamic torque are calculated.

The drive train is modeled as proposed in [6], where the structural model is explained by mass, spring/damper model. The model consists of the following components:

- The combined rotational moment of inertia I_r of the rotor and low-speed shaft.
- A viscous damper with viscosity constant B_r representing the bearings in the low-speed part of the drive train (before the gear box).

- A massless, viscously damped rotational spring with spring constant K_d and viscosity B_d . The spring deformation θ , measured in radians, represents the deformation of the low-speed shaft.
- A gearbox with ratio N_g .
- A viscous damper with viscosity constant B_g representing the bearings in the high-speed part of the drive train (after the gear box).
- The combined rotational moment of inertia I_g of the gearbox, high-speed shaft, and the generator.

The combined differential equations describing this system are:

$$\begin{aligned}
I_r \dot{\omega}_r &= T_a - K_d \theta - B_d \left(\omega_r - \frac{\omega_g}{N_g} \right) - B_r \omega_r \\
I_g \dot{\omega}_g &= -T_g + \frac{K_d}{N_g} \theta + \frac{B_d}{N_g} \left(\omega_r - \frac{\omega_g}{N_g} \right) - B_g \omega_g \\
\dot{\theta} &= \omega_r - \frac{\omega_g}{N_g}
\end{aligned} \tag{5}$$

where, the aerodynamic torque T_a and the generator torque T_g are the inputs to the system, and the resulting rotational speeds of the rotor and the generator, denoted ω_r and ω_g , are outputs. As (5) constitutes a system of coupled, linear differential equations, they readily lend themselves to a linear state-space representation.

The tabular steel tower will be deflected in the fore-aft direction due to the thrust force on the rotor. A simple model approximates the deflection with a linear displacement of the nacelle, with the dynamics described by

$$m_t \ddot{z} = -K_t z - D_t \dot{z} + F_t, \tag{6}$$

where z , \dot{z} , and \ddot{z} are position, velocity, and acceleration of the nacelle respectively, and m_t , K_t , and D_t are constant coefficients of the linear model (They can also be seen as the mass, stiffness, and damping parameters of the tower respectively).

We will consider the generator as a component that attempts to deliver the electrical power P_e specified by the power reference signal P_0 . The power is controlled by adjusting the rotor current, which in turn, governs the amount of torque exerted by the generator to the high-speed shaft. Further, we will assume a loss-less generator, meaning that the electrical power equals the product between the generator speed and the generator torque:

$$P_e = \omega_g T_g. \tag{7}$$

Practical generators cannot change the torque instantaneously. We will model this latency by a first order relationship between the requested generator torque and the actual generator torque as [6, 8]

$$\dot{T}_g = \frac{1}{\tau_g} (T_{g,ref} - T_g), \tag{8}$$

where τ_g is the time constant in this formulation. As the desired torque is given by $T_{g,ref} = \frac{P_0}{\omega_g}$, we have

$$\dot{T}_g = \frac{1}{\tau_g} \left(\frac{P_0}{\omega_g} - T_g \right) \tag{9}$$

Thus, (7) and (9) leaves the generator as a nonlinear first order system with the generator speed ω_g and the generator power set point P_0 being the inputs, and with the generator torque T_g and the produced power P_e being the outputs.

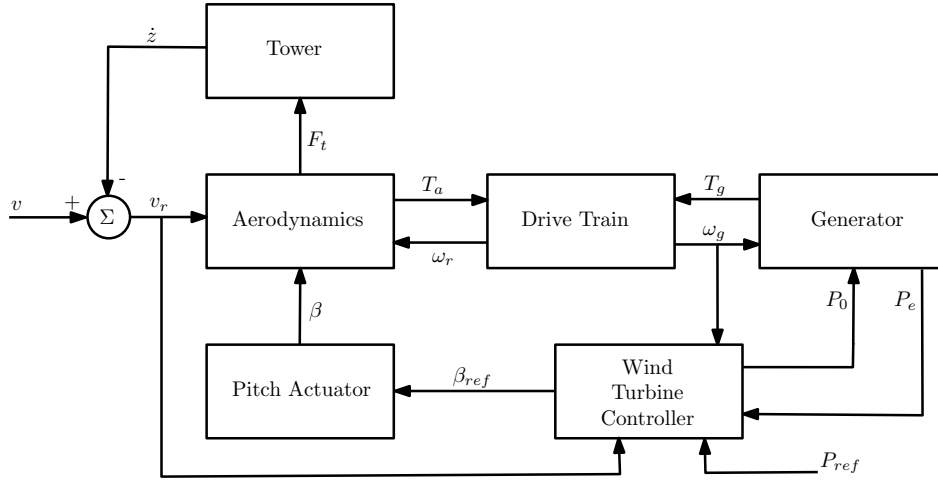


Figure 2: The block diagram of the single wind turbine model.

The system providing blade pitch angle control consists of a electrical or hydraulic drive, gears, and electronic control circuits. Thus, developing a detailed model of the pitch system is exhaustive, and we approximate it to the model proposed in [6]. That is a first order system with a time delay. We will use the following first order relation between the pitch angle reference β_{ref} and the actual blade pitch angle β [6, 8]:

$$\dot{\beta} = \frac{1}{\tau_{\beta}}(\beta_{ref} - \beta), \quad (10)$$

where τ_{β} is the time constant of the pitch actuator. Besides, a rate limit of $\pm 20 \frac{deg}{s}$ is considered for β .

A simple wind turbine controller is used which is basically a switching of the controller between full load and partial load controller based on the wind speed measurement. The full load controller is a gain-scheduled PID which measures the generator speed ω_g and acts on the pitch reference β_{ref} in order to keep the generator speed at the nominal speed. The partial load controller set β_{ref} to the (constant) optimal point and applies a PID controller on the generator power set point P_0 using the measurement of ω_g either to prevent the generator speed to exceed the maximum speed or to keep the turbine operating on the optimal power curve. In both cases, the upper bound of the generator power set point is the power reference P_{ref} , which is determined by the wind farm controller.

3.2 Fatigue Load

The most correct method for calculating the fatigue load is rain flow counting [3, sec. 5.9.5]. It is not even a mathematical function. It is an algorithm and it is then very non linear. It can be used as a post processing algorithm in the simulation program. For example fatigue loads related to tower position, gear box twist, collective rotor torque and pitch acceleration or speed can be calculated with this method. However, for control design models and also for simpler simulation models a simpler approximation will be useful. Therefore a number of suggestions are listed below.

Standard deviation: This measure is not affected by the mean value which complies with fatigue load. If Φ_x is the power spectrum for x the standard deviation (11) integrates all amplitudes disregarding their frequency. This means that standard deviation is not affected by the frequency contents

which does not at all comply with fatigue load.

$$std(x) = \sqrt{\int_{-\infty}^{\infty} \Phi_x(\omega) d\omega} \quad (11)$$

Using the Wöhler curve: If the Wöhler curve is inserted in the Palmgren-Miner sum (see [6]) the measure (12) is obtained. This suggests the approximation of (13) based on the power spectrum for x . Notice that $\Phi_x^{1/2}$ represents the amplitude at frequency ω , and when multiplied with ω the number of cycles in time is added up to the average fatigue load increase in time.

$$D = \sum_i \frac{n_i}{N_i} = \sum_i \frac{n_i}{kS_i^{-m}} = k^{-1} \sum_i n_i S_i^m \quad (12)$$

$$D_S = k^{-1} \int_{-\infty}^{\infty} \omega \Phi_x(\omega)^{\frac{m}{2}} d\omega \quad (13)$$

where n_i is the number of cycles with amplitude S_i , N_i is the fracture number of cycles, and k and m are the material parameters found in the handbooks. **Standard deviation for derivative:** If this is used for a signal x the measure (14) is obtained. As $\Phi_x^{1/2}$ represents the amplitude at frequency ω this is a good measure for Wöhler exponent 2 except the weight is ω^2 corresponding to squared number of cycles, compare also with (12) and (13).

$$std(\dot{x}) = \sqrt{\int_{-\infty}^{\infty} \omega^2 \Phi_x(\omega) d\omega} \quad (14)$$

3.3 Wind Field

The wind field model simulates the wind speed at wind farm grid points in two dimensions. The model includes the ambient turbulent two dimensional wind field, wakes meandering behind turbines, wakes dependence on the turbine thrust and thereby power, and the merging of wakes. Presently, it does not include the added wake turbulence.

Ambient wind field: The ambient wind field model is developed so that for a given mean wind speed, turbulence intensity, lateral displacement, number of lateral points/channels, number of time samples and sampling time:

- Two spectral matrices are formed for longitudinal and lateral wind speed respectively. These matrices also depend on additional parameters e.g. length scale and coherence decay which is considered constant but the value can be changed in the program.
- Based on these spectra the model simulates longitudinal and lateral wind speed in a grid consisting of the number of lateral points with the given displacement and longitudinal points with displacement mean wind speed times sampling time.

To simulate wind speeds in a horizontal grid with a given longitudinal and lateral spacing, the straight forward approach would be to generate a stochastic process for each grid point. However, assuming Taylor's frozen turbulence hypothesis for inviscid flow [4, p. 49] to be true it is only necessary to simulate stochastic processes in the first line in the lateral direction in the park. These velocities are then assumed to travel with the average wind speed in the longitudinal direction. In this way the wind speeds at downwind grid points will eventually be generated.

To simulate the ambient wind speed a program has been developed. In short, it follows the following steps:

1. Generates the covariance from the spectral matrix by the Kaimal spectrum in accordance with the latter standard chosen from [3, p 23-25] and coherence decay parameter [15, section 9.4].
2. Generate the amplitudes from the covariance.
3. Generate the vector time series by using FFT.

Wake deficit: The wake deficit and expansion modeled by [5] is based on momentum approach under the assumptions of constant eddy viscosity in the wake and self-similarity of the wake flow speed deficit and turbulence is used in the simulation model. It is concluded in [5] that the wake area expansion can be obtained by

$$\frac{A(x)}{A(0)} = \left(\beta_s^{\frac{k}{2}} + 2\alpha_s \frac{x}{R} \right)^{\frac{2}{k}}, \quad (15)$$

where $A(0)$ is the wake area at the turbine, $A(x)$ is the wake area by the distance x behind the rotor, $k = 3$ is chosen as the Schlichting factor ([5] proposes $k = 2$. [10] and [12] propose $k = 1$), the constant α_s and β_s can be determined experimentally. The wind speed is then approximated by

$$\frac{u(x)}{u(0)} = 1 - \frac{1}{2} C_T \frac{A(0)}{A(x)}, \quad C_T < 1 \quad (16)$$

where $u(x)$ is the wind speed at distance x down stream and $u(0)$ is the wind speed at the turbine.

Wake meandering: Wake meandering explains how the wake displacements can be modeled along the mean wind speed direction (see [14]). In this mechanism, the dynamic wake flow from the upstream wind turbine is superimposed by the wake deficit of that wind turbine on the ambient wind field.

The most important assumption to be considered in the wake meandering is that the displacement of the wake is the result of the large-scale air movements and that the turbulence diffusion is less important. In fact, the main idea of the meandering model is that the transport of the wake deficit acts as a passive tracer disregarding its own momentum. The Taylor's hypothesis basically describes the situation in wake meandering, in which the down stream advection is controlled by the mean wind speed of the ambient wind field so the wake momentum in the mean wind flow direction is invariant with respect to the prescribed longitudinal wake displacement. Thus, the mutual interaction of wake momentum and wake displacement is neglected in the model.

3.4 Wind Farm Controller

The simulation model uses a simple way for distributing the farm active power references to all wind turbines which is according to the proportional distribution [11]. The reference will be calculated by

$$P_{ref_i} = P_{demand} \cdot \frac{P_{avail_i}}{P_{avail}}, \quad (17)$$

where P_{ref_i} is the power reference (set point) for the i th wind turbine, P_{demand} is the requested active power from the network operator, P_{avail_i} is the available power at the i th wind turbine obtained from the wind speed measurement by equation (1), and P_{avail} is the total available power at the farm by $P_{avail} = \sum_{i=1}^n P_{avail_i}$, where n is the number of wind turbines in the farm.

3.5 Network Operator

The network operator model is used as an interface to connect the wind farm to the electrical grid. The grid requirements are assigned manually as inputs of the network operator. Besides, there is an

extra input to this model which gives an estimation of the available power at the farm. The output of the network operator is the active power demand.

Possible scenarios for the wind farm are taken into account when the wind farm contribute to the grid and works as a power plant [2, 8]. In the simulation model, five different modes for this contribution are considered as:

- Absolute active power control, where the network operator asks the wind farm controller to produce a specific amount of power. This happens when the transmission capability of the grid decreases due to some malfunctions and etc. A prediction of the available power is a feedback from the wind farm controller to the network operator which can determine the maximum power that can be produced in the farm.
- Frequency control, where the wind farm contributes to the frequency regulation of the grid by increase or decrease of the produced power. In this case, the network operator has to measure the frequency in the grid and assign a dead-band control to the power production.
- Delta mode, where the operator asks the wind farm controller to reserve Δ amount of available power as given by the prediction of the available power from the wind farm controller. This actually means that the operator requests a power reserve. In [7] it is mentioned that the reserve power could be used for frequency control.
- Power rate limiter, where the operator asks to limit the rate of the power increase. This happens when the wind farm faces a predicted storm or high wind speed and the network operator would like to limit the variations of the power.
- Balance control, where the network operator adjusts the wind farm production in order to meet the contract volume of the power generation of the available power systems [16]. Wind power represents a variable generation source because of changes in the wind conditions. In this mode, the operator asks the wind farm controller to decrease or increase the production at specific levels. This mode of the power demand can basically interpreted similar to the active power control.

4 Simulation Results

Offshore Windpark Egmond aan Zee (OWEZ, located in The Netherlands) consists of 36 turbines. Data for six turbines in the southern corner of the park is available for evaluation. The spatial grid resolution of 5 meters is considered for a simulation area of the width of 2500 meters and the length of 2000 meters. The simulation time of 1000s is considered where the dominant wind blows from west to east. The dark red points in the image represent the higher speed of the longitudinal wind at those points (Consequently, blue points represent the lower wind speed). The mean wind speed (in selected data segment) of the WT4 (about $9(\frac{m}{s})$) is considered as the ambient mean wind speed. The turbine parameters of Vestas V90 is used in the simulation model and the individual wind turbines are set to the power reference of 3000KW.

As it is shown in figure 3, WT14 and WT15 are in the wake of the WT3 and WT4. Consequently, a wind speed reduction is expected in WT14 and WT15. Figure 4 shows the mean wind speed comparison of the simulated farm and real data farm. Both real and simulated data show the wind speed reduction on WT14 and WT15. It also shows that the wake deficit in reality is more than the simulation. The simulation results do not show a significant deficit on WT16 mean wind speed. This is due to the fact that WT16 is not in the wake of any of simulated wind turbines in the simulation. However, in reality, WT16 is in the wake of WT5 which will result in mean wind speed reduction on WT16.

Note that this comparison is a static analysis while the model is subject to be used for dynamic simulation. Therefore the next step of investigations will be the dynamic verification of the model.

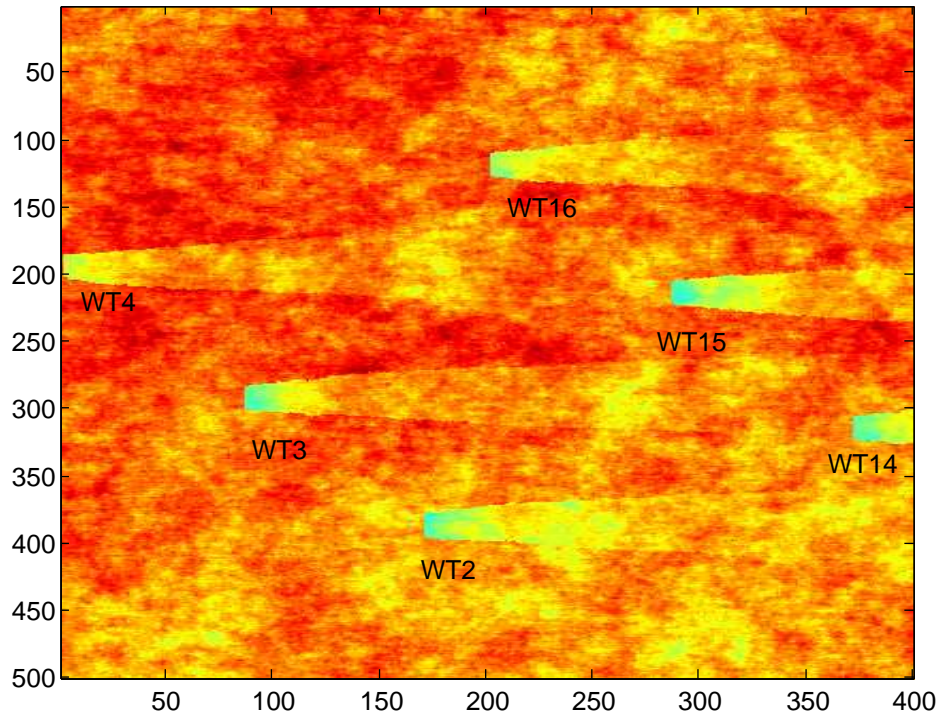


Figure 3: The simulation of the wind flow in OWEZ farm (The units of the axis are 5 meters. e.g., the stream-wise distance is 2000 meters.).

References

- [1] Aeolus (2008). Distributed control of large-scale offshore wind farms. <http://www.ict-aeolus.eu>.
- [2] Bjerge, C. and J. R. Kristoffersen (2007). Run an offshore wind farm like a power plant. *VGB PowerTech* (4), 63–66.
- [3] Burton, T., D. Sharpe, N. Jenkins, and E. Boassanyi (2008). *Wind Energy Handbook* (second ed.). John Wiley & Sons, Ltd.
- [4] Davidson, P. A. (2004). *Turbulence*. Oxford University Press.
- [5] Frandsen, S., R. Barthelmie, S. Pryor, O. Rathmann, S. Larsen, J. Højstrup, and M. Thøgersen (2006). Analytical modelling of wind speed deficit in large offshore wind farms. *Wind Energy* 9, 39–53.
- [6] Hammerum, K., P. Brath, and N. K. Poulsen (2007). A fatigue approach to wind turbine control. *Journal of Physics: Conference Series* 75, 012081 (11pp).
- [7] Hansen, A. D., P. Sørensen, F. Iov, and F. Blaabjerg (2006a). Grid support of a wind farm with active stall wind turbines and ac grid connection. *Wind Energy* 9, 341–359.

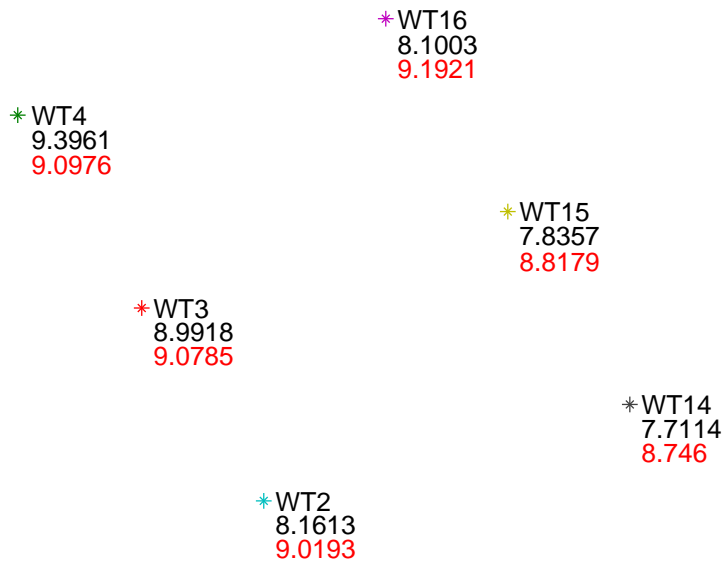


Figure 4: Comparison of mean wind speed during 1000s on 6 wind turbines from OWEZ. Black numbers are achieved from measurement and Red numbers are obtained from simulation

- [8] Hansen, A. D., P. Sørensen, F. Iov, and F. Blaabjerg (2006b). Power control of a wind farm with active stall wind turbines and ac grid connection. In *European Wind Energy Conference and Exhibition*.
- [9] Hansen, M. O. L. (2008). *Aerodynamics of Wind Turbines* (second ed.). Earthscan. USA.
- [10] Jensen, N. (1983). A note on wind generator interaction. Technical report, Risø National Laboratory, Roskilde.
- [11] Kaneko, T., T. Senjyu, A. Yona, M. Datta, T. Funabashi, and K. Chul-Hwan (2007, Nov.). Output power coordination control for wind farm in small power system. *Intelligent Systems Applications to Power Systems, 2007. ISAP 2007.*, 1–6.
- [12] Katic, I., J. Højstrup, and N. Jensen (1986). A simple model for cluster efficiency. In *European Wind Energy Conference and Exhibition*.
- [13] Knudsen, T., T. Bak, and M. Soltani (2009). Distributed control of large-scale offshore wind farms. In *European Wind Energy Conference and Exhibition (EWEC) 2009*. European Wind Energy Association (EWEA). http://www.ewec2009proceedings.info/allfiles2/246_EWEC2009presentation.pdf.
- [14] Larsen, G. C., H. A. Madsen, K. Thomsen, and T. J. Larsen (2008). Wake meandering: a pragmatic approach. *Wind Energy* 11(4), 377–395.
- [15] Panofsky, H. A. and J. A. Dutton (1984). *Atmospheric Turbulence*. John Wiley & Sons.
- [16] Suwannarat, A., B. Bak-Jensen, and Z. Chen (2006). Power system balancing with large scale wind power integration. In *Sixth International Workshop on Large-Scale Integration of Wind Power and Transmission Networks for Offshore Wind Farms*.